UDC 541.515; 547.413; 544.175

DYNAMICS OF HINDERED CF_3-ROTOR IN 2,5-BIS(TRIFLUOROMETHYL)NITROBENZENE RADICAL-ANION IN ANHYDROUS DMF. A TEMPERATURE-ACTIVATION THEORY OF REVERSIBLE HFS TRANSFORMATIONS OF EPR SPECTRUM

E.A. Polenov, P.V. Melnikov@

Moscow Technological University (Institute of Fine Chemical Technologies), Moscow, 119571 Russia
@Corresponding author e-mail melnikovsoft@mail.ru

The temperature dependence of EPR spectrum of 2,5-bis(trifluoromethyl)nitrobenzene radical anion in anhydrous DMF was investigated. Internal dynamics of hindered rotation of the CF_3-group in ortho-position to NO_2-group causes HFS modulation. The spectrum changes are reversible and temperature-dependent. An original temperature-activation representation of complex spectral density was proposed instead of the traditional spectral-kinetics representation to explain the observed transformation. The change resulted in a new convenient phenomenological reconstruction model, which allowed simulating the spectra in the whole temperature range. Splitting constants and contributions to the spectral widths of the spectral lines were found. The activation energy of the CF_3-group hindered rotation is significant and amounts to 37 kJ/mol.

Keywords: *radical-anion, spectra simulation, dynamic modulation, spectral density.*

Introduction

Temperature-reversible transformations of the EPR spectrum of a free radical (FR) are almost the only source of experimental information about its low-frequency (~10^6–10^8 s^{-1}) internal motion.

Anion radicals (AR) are optimal objects for studying temperature-dependent hyperfine structure (HFS) due to the features of stereospecific hyperfine interactions (HFI) in π-radicals containing fluoroalkyl substituents, because the observed HFI constants are the greatest of possible in the charge triad [1, 2].

Previously we have studied the spectra of anion radicals of *ortho*-nitrobenzotrifluoride 2-CF_3-C_6H_4-$NO_2^{\bullet}$ (AR I) in N,N'-dimethylformamide (DMFA) and acetonitrile [3, 4] and of 2,5-bis (trifluoromethyl)nitrobenzene 2,5-$(CF_3)_2$-C_6H_3-$NO_2^{\bullet}$ (AR II) in acetonitrile [5]. Both ARs show a strong dynamic modulation (DM) of the HFS in the EPR spectrum caused by the constrained hindered torsion and deformation motions of the CF_3 and NO_2 groups with an extreme activation barrier (~ 34.7 kJ/mol) in aprotic solvents. The reversibly transformed spectral contour maintains very high characteristicity when scanning temperature. AR II differs from its analog AR I only in the second CF_3 group freely rotating in the *meta* position and represented in the EPR spectrum by a binomial quartet with a small splitting constant.

* Original Russian Text © E.A. Polenov, P.V. Melnikov, 2016, published in Tonkie Khimicheskie Tekhnologii / Fine Chemical Technologies, 2016, Vol. 11, No 3, pp. 31–38.

We found that the spectral and kinetic mode and the barriers of the internal hindered rotation of the CF_3 rotor and rotational diffusion depend on the composition of the mixed solvent in the liquid mixture DMFA-water for AR I. Because the HFS maintains high characteristicity in the mixtures, the AR showed the properties of an effective spin probe allowing to find signs of stoichiometric structuring in the mixed solvate cage [6].

The results of [3, 4, 6] allowed to correct a number of essential mistakes made previously by researchers when interpreting the EPR spectra of AR I [7, 8]. The mistakes were caused by the imperfection of the former equipment, the absence of the HFI theory, the small amount of the obtained primary information and the absence of a planned experiment with consecutive scanning of temperature. The type of the HFS is in conflict with the hypothesis of equivalence of ^{19}F nuclei, and its parameters presented in [7, 8] without clarification of the mode of dynamic modulation are not proved, including even the constant of fluorine splitting.

In this work the reversible transformation of the EPR spectrum of AR II in DMFA was studied. Besides, a version of the theory of reversible transformations of HFS was suggested with the participation of previously obtained data. This allows creating a uniform phenomenological model for the reconstruction of the spectral contour in the whole experimentally attainable range of temperature-reversible dynamic transformation of the spectral contour modeled by the superposition of Lorentz resonant lines.

Experimental

High purity DMFA was stored in a bottle with two ground glass joints over molecular sieves with 3 Å pores and distilled in vacuum shortly before measurements.

2,5-Bis(trifluoromethyl)nitrobenzene was purified before measurements by vacuum distillation. Its solution in anhydrous DMFA was subjected to several cycles of degasification in vacuum at 10^{-3} torr, and the vessel with the ready anaerobic solution was filled with a spectrally pure inert gas.

AR II was obtained by the reaction of one-electron transfer from potassium *tert*-butylate C_4H_9OK.

EPR spectra were recorded in the range $207 \leq T \leq 290$ K with the use of a modernized digitized EPR-V X-range radio spectrometer with a temperature attachment. Each spectrum is a numerical array of 4096 points. Processing was carried out in a program complex [9] created by us. The selection of a reconstruction model and the determination of its optimum parameters was described previously in detail in [3–5]. For the reconstruction we used the phenomenological model of HFS in the form of superposition of nondegenerate Lorentz lines of separate resonant transitions constructed on the basis of the low-temperature limit form (LF). This model takes into

account the shifts and broadenings of the nondegenerate components of the fluorine Fermi-contact multiplet (FCM) of the HFS in the course of temperature scanning.

Examples of the registered EPR spectra (on the left) and their reconstruction (on the right) are presented in Figure 1. The HFS model takes into account the dipolar broadening of the components of the nitrogen triplet and the exchange broadening of the components of the fluorine multiplet of the CF_3 group in the *ortho* position. The calculated parameters of the HFS are presented in the table.

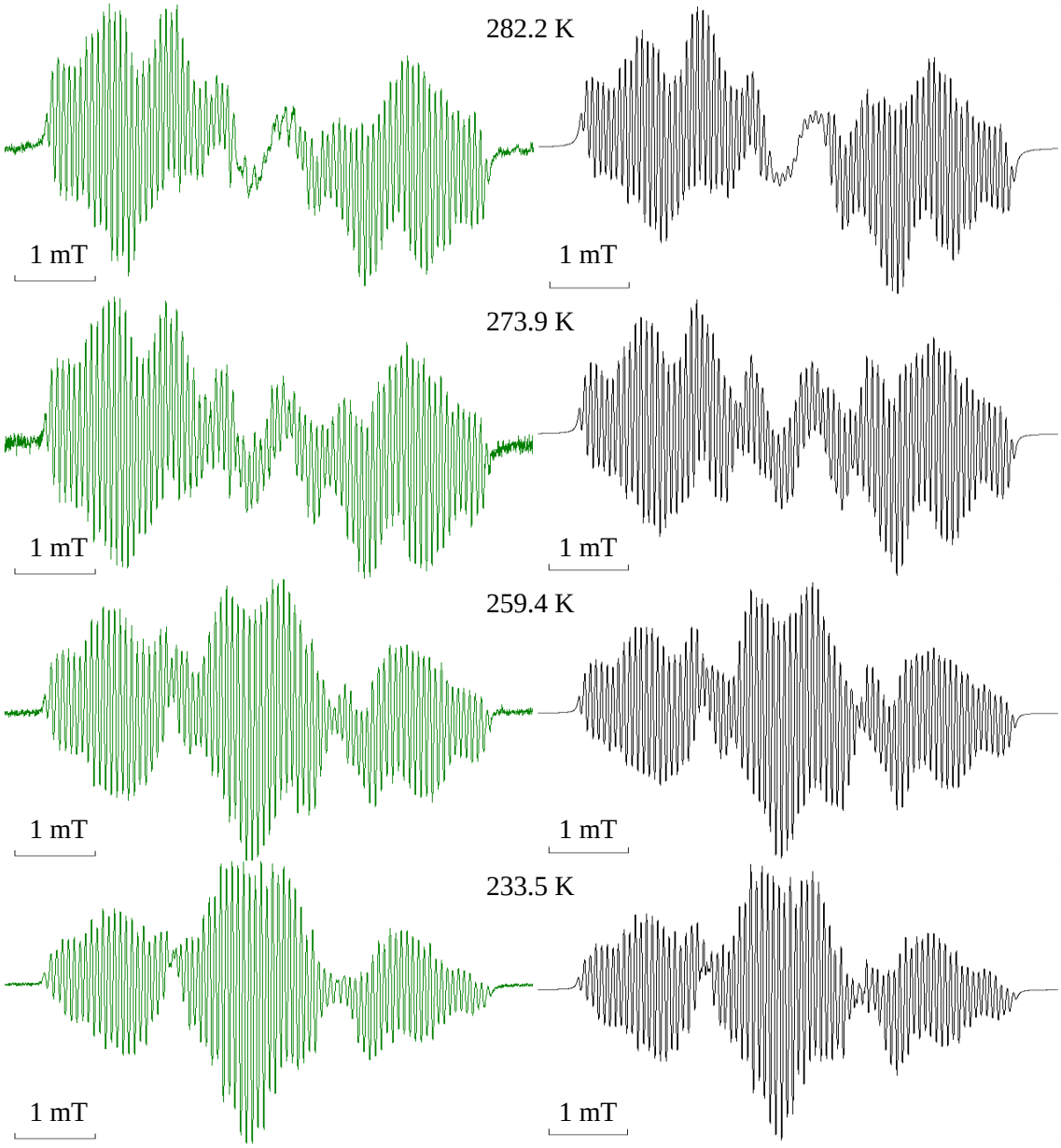

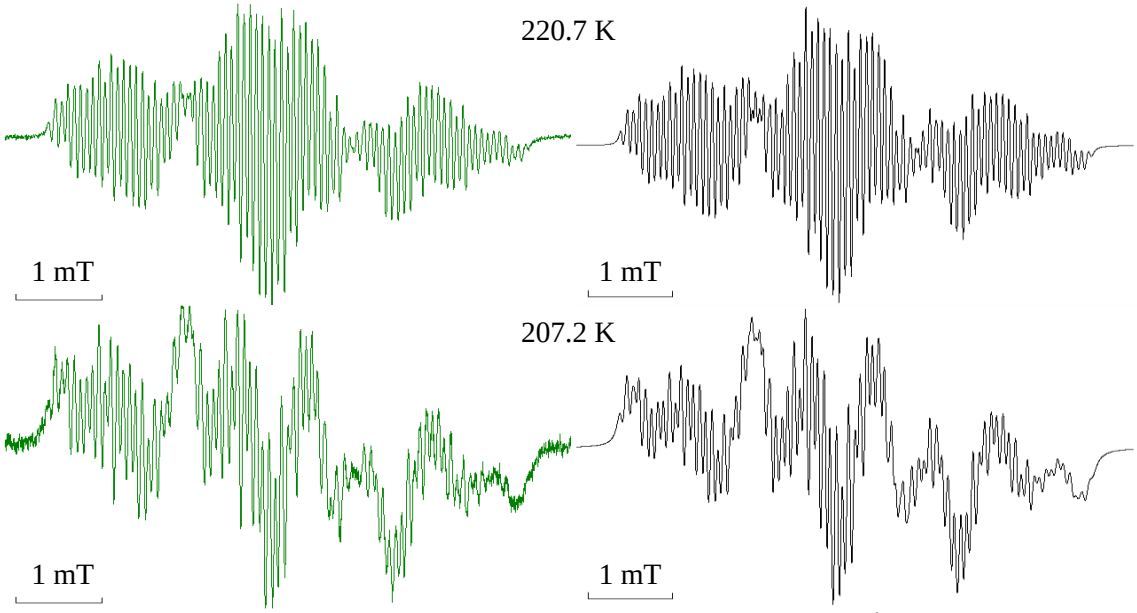

Figure 1. Examples of EPR spectra of AR 2,5-$(CF_3)_2$-C_6H_3-$NO_2^{\bullet-}$ (on the left) and their reconstructions (on the right) in anhydrous DMFA.

Hyperfine splitting constants and dynamic contributions in the broadness of lines (mT) in the EPR spectrum of AR II at different temperatures

T, K	a_{F1}	a_{F2}	a_{F3}	a_N	a_{Hp}	a_{Ho}	$a_{Hм}$	$a_{Fм\text{-}CF3}$	Γ_0	$W_{N(+1)}$ $\times10^3$	$W_{N(-1)}$ $\times10^3$	$j_{F(mi)}$ $\times10^3$
290.0	1.4359	1.4359	0.1831	0.6267	0.4933	0.2723	0.1412	0.0674	0.0345	1.0	1.7	64.7
282.3	1.4528	1.4528	0.1528	0.6294	0.4918	0.2740	0.1405	0.0692	0.0354	–0.1	1.1	44.2
278.2	1.4670	1.4670	0.1212	0.6295	0.4932	0.2756	0.1402	0.0693	0.0301	0.5	1.9	22.3
273.9	1.4713	1.4713	0.1158	0.6333	0.4948	0.2775	0.1394	0.0705	0.0293	0.1	1.9	15.8
273.9*	1.4723	1.4723	0.1092	0.6345	0.4935	0.2781	0.1381	0.0728	0.0317	–1.6	–0.7	11.6
267.5	1.4729	1.4729	0.1110	0.6341	0.4948	0.2780	0.1380	0.0728	0.0298	–1.1	1.3	11.8
263.4	1.4747	1.4747	0.1083	0.6357	0.4936	0.2790	0.1372	0.0735	0.0301	–2.4	0.4	6.7
259.4	1.4766	1.4766	0.1072	0.6364	0.4938	0.2793	0.1365	0.0734	0.0304	–2.2	0.9	3.9
255.6	1.4781	1.4781	0.1065	0.6373	0.4936	0.2803	0.1367	0.0742	0.0309	–2.4	1.0	1.5
251.9	1.4783	1.4783	0.1046	0.6381	0.4935	0.2809	0.1365	0.0763	0.0312	–2.5	1.6	0.8
247.7	1.4778	1.4778	0.1030	0.6387	0.4923	0.2812	0.1364	0.0770	0.0326	–2.9	1.7	0.6
237.7	1.4776	1.4776	0.1015	0.6393	0.4917	0.2816	0.1367	0.0779	0.0309	–2.5	3.1	–0.5
233.5	1.4783	1.4783	0.1009	0.6395	0.4920	0.2821	0.1366	0.0786	0.0319	–2.5	3.8	–0.4
230.2	1.4803	1.4803	0.1002	0.6405	0.4931	0.2829	0.1364	0.0791	0.0343	–3.6	3.5	–0.3
226.5	1.4805	1.4805	0.0983	0.6419	0.4907	0.2831	0.1363	0.0798	0.0330	–2.3	6.2	–0.3
220.7	1.4822	1.4822	0.0973	0.6435	0.4914	0.2836	0.1363	0.0806	0.0335	–1.9	7.9	0.5
216.1	1.4836	1.4836	0.0958	0.6436	0.4915	0.2844	0.1380	0.0816	0.0368	–2.8	8.4	–0.3
211.7	1.4844	1.4844	0.0967	0.6430	0.4917	0.2848	0.1356	0.0823	0.0438	–5.1	7.1	0.0
207.2	1.4828	1.4828	0.0923	0.6442	0.4881	0.2850	0.1390	0.0839	0.0484	–1.8	13.8	0.8

* After a steep rise from the low temperature range (test for reproducibility - reversibility).

Results and Discussion

The model contours of HFS are in very good agreement with the experimental ones. The nature of minimal differences is due to the used equipment and is associated with the very small delay of registration of the numerical array forming the absorption contour with respect to the speed of its scanning.

The qualitative picture of temperature-dependent transformations of the EPR spectra of AR II is similar to that found by us previously for AR I [3], because it is generated by the common structural fragment. The first mechanism, the basic one, is associated with the torsion movement of the CF_3 rotor adjacent to the nitro group, and is shown in shifts and broadening of six of eight components of the phase-shift-code keyed signal [4]. The second mechanism of temperature changes of the HFS, as in the solutions of the ARs of all nitroarenes, is due to rotational diffusion and manifests itself as the asymmetric deformation of the lines of the nitric triplet ^{14}N. For its description the simplest model of spherical rotational diffusion turned out to be quite sufficient.

As a rule, interpretation of HFS is associated with the circular frequency ω and the time τ of correlation of the movement. These parameters play the role of a spectral-kinetic (SK) couple of arguments in the spectral display of the simplified kinetic model of the dynamics of the stationary random process. Temperature plays the key role in the organization of the physico-chemical laboratory experiment. However, it is introduced via the activation Arrhenius equation as a part of correlation time τ, and it is a hidden variable. As a result, temperature correlations are used instead of analytical presentation of spectral measurements data. This is unacceptable and must be corrected.

The DM of a Fermi-contact HFS manifests itself as broadening and shifts of the resonant lines of the multiplet of the nuclei of a mobile group of chemically equivalent atoms (GCEA). It is one of the most conspicuous mechanisms of temperature changes in the EPR spectrum of a free radical in solution. On the boundaries of the ideal (in general not attainable) temperature range the multiplet of GCEA nuclei, as well as the spectrum in general, take one of LFs. An equilibrium (**E**) LF corresponds to the "static" orientation of the nuclei and an extremely long time of the movement correlation ($\omega\tau >> 1$). A dynamic LF (**R**) arises when superfast movement is attained at $\omega\tau << 1$. Changes of conditions perturb the LF, and a chain of the dynamic phases (DP) arises. A mental experiment allows to separate the main DPs generated by counter thermal agitations of both LFs.

The low-temperature side of the chain shows LF **E** and then the DP of slow (**S**) movement. The high-temperature side has LF **R** and the DF of fast (**F**) movement (in NMR "exchange"). So, the multiplet on the sides changes as (**E↔S**) or (**F↔R**), and these schemes are invariable up to the transitional (**I**) range ($\omega\tau \sim 1$). In the center of the range the shifting lines are maximally broadened. The range in general is divided into ranges as **E↔S↔I↔F↔R**, and, if necessary, it can be described with any level of detail. For example, fragment …↔**(S)I↔I↔I(F)**↔… arises near the center of the chain of phases, and the detailed chain of DM phases (PDM) takes the following form:

$$\mathbf{E}\leftrightarrow\mathbf{S}\leftrightarrow(\mathbf{S})\mathbf{I}\leftrightarrow\mathbf{I}\leftrightarrow\mathbf{I}(\mathbf{F})\leftrightarrow\mathbf{F}\leftrightarrow\mathbf{R}, \quad (1)$$

if one isolates all characteristic transforms of the HFS in the form of PDM. In ranges **E↔S** and **F↔R** the simplified schemes of HFS reconstruction on the basis of the perturbed LF are effective, but in area **I** they are no longer adequate. Limit schemes are sufficient for most hydrocarbonic radicals, but for organofluorine systems it is desirable to supplement the theory.

Let us perform transition to the temperature-activation (TA) representation of the HFS parameters using a minimum of symmetrizing transformations of the real $j(\omega\tau)$ and imaginary $k(\omega\tau)$ components of complex spectral density (CSD), in which the dimensionless product of resonant circular frequency ω and correlation time τ is taken as uniform spectral-kinetic argument Y:

$$Y = \omega\tau. \quad (2)$$

$$j(Y) = (g_0/\omega)\times Y/[1+Y^2], \quad (3)$$

$$2j_0 = g_0/\omega, \quad (4)$$

$$k(Y)=Y\times j(Y). \quad (5)$$

Let us take into account the activation Arrhenius equation for correlation time:

$$\tau=\tau_\infty\times\exp(E\times T^{-1}). \quad (6)$$

Let us write:

$$Y = (\omega\tau_\infty)\times\exp(E\times T^{-1}). \quad (7)$$

Let us introduce the dimensionless substitution:

$$\omega\tau_\infty=\exp(-E\times T_0^{-1}). \quad (8)$$

Let us represent inverse temperature as a sum:

$$T^{-1} = \theta + \theta_0 \quad (9)$$

isolating the reference point of temperature argument $\theta_0 = T_0^{-1}$. Then equation (2) is transformed to equality (10) providing the substitution of arguments:

$$Y = \omega\tau = \exp(E\times\theta). \quad (10)$$

Equations (3) and (5) take a compact form based on hyperbolic functions:

$$j(Y) = 2j_0\times Y^{-1}Y\times (Y^{-1}+Y)^{-1}= j_0\times\mathrm{ch}(E\times\theta)^{-1}, \quad (11)$$

$$k(E\times\theta) = j_0\cdot\exp(E\times\theta)\times\mathrm{ch}(E\times\theta)^{-1}= j_0\times [1+\mathrm{th}(E\times\theta)]. \quad (12)$$

It is expedient to represent the imaginary component of complex spectral density (12) containing two summands as a scalar product of a pair of two-component vectors:

$$\mathbf{E} = \{1, 1\},$$

$$\mathbf{T} = \{1, \mathrm{th}(E\times\theta)\}, \quad (13)$$

$$k(E\times\theta) = j_0\times(\mathbf{E}\bullet\mathbf{T}) = j_0\times(\{1, 1\}\bullet\{1, \mathrm{th}(E\times\theta)\}).$$

Subsequent simple replacement of unit vector **E** with scale-calibrating vector **A** gives the temperature function of splitting constants (34), which is theoretically derived on the basis of stationary kinetics of activation supply of thermal maintenance of equilibrium.

The logarithm of the real component of spectral density (11) forms an illustration of temperature changes of spectral density. The asymptotes of its sides are two infinitely divergent half-lines (Figure 2) (for $\lambda = 0$), and the extreme absolute values of their slope coefficients are equal to activation energy:

$$\lim_{\theta\to\pm\infty} d(\ln j(E\times\theta))/d\theta = \pm E\,. \qquad (14)$$

However, the EPR spectrum of AR II in DMFA even at 250 K shows pronounced full braking of the CF_3 rotor adjacent to the NO_2 group, which generates a plateau in the bottom of the curve of $\ln j_F\,(T^{-1})$ (Figure 3) not observed previously in case of AR I. It is easy to imitate the effect by means of a small perturbation of λ.

Let us designate the perturbed function of real spectral density by $j_1(\theta)$:

$$j_1(\theta) = ch^{-1}(E\times\theta) + \lambda \qquad (15)$$

and compare the logarithms:

$$\ln j_0(\theta) = \ln[ch^{-1}(E\times\theta)], \qquad (16)$$

$$\ln j_1(\theta) = \ln[ch^{-1}(E\times\theta) + \lambda]. \qquad (17)$$

This gives the asymptotic limit of perturbed spectral density in the low-temperature side:

$$\lim_{\theta\to+\infty} \ln j_1(\theta) = \ln\lambda \;\; \ln j_1(\theta) = \ln \square. \qquad (18)$$

Subtracting (18) from (17) to compensate the perturbation we obtain expressions $\ln j_2(\theta)$ and $j_2(\theta)$ equivalent to $\ln j_1(\theta)$ and $j_1(\theta)$, but displaced along the ordinate axis:

$$\ln j_2(\theta) = \ln[ch^{-1}(E\times\theta) + \lambda] - \ln\lambda; \qquad (19)$$

$$j_2(\theta) = \lambda^{-1} ch^{-1}(E\times\theta) + 1. \qquad (20)$$

Model curves $\ln j$ and $\ln j_1$ for different values $\lambda\times10^4 = 0, 1, 2, \ldots 8$ are shown in Figure 2.

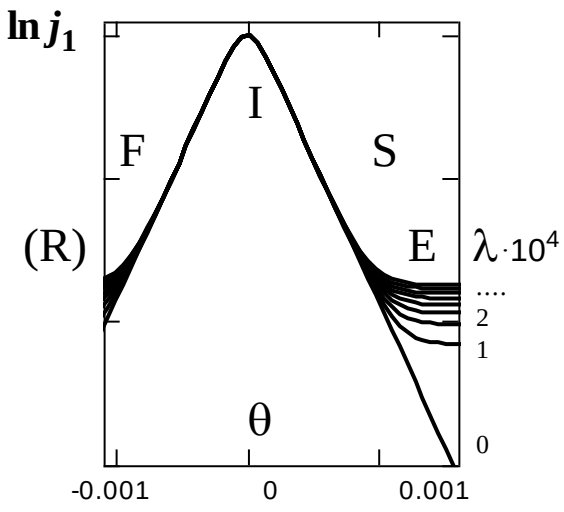

Figure 2. Modelling the real component of complex spectral density *j* (broadening) upon perturbation by small parameter λ and the range of dynamic modulation.

They are undistinguishable in the range **F↔I↔S**, but differences arise in the range **S↔E**, and curve $\ln J_1(\theta)$ takes the shape of a "hockey stick" with a base sensitive to parameter λ (Figure 2). This allows isolating a point of transition to the "static" range **E**, the nature of which can be various. Functions (15) and (20) are more realistic than customary (11). However, being an evident illustration of classification of spectral-kinetic ranges (1) of the temperature interval they are limited to the experimental conditions. When $\theta > 0$ (low temperatures), the range limit is the solution freezing point. When at $\theta < 0$ (high temperatures), a kinetic limit arises, if the studied

radical particle loses stability. The more distant inevitable thermodynamic limit coincides with the solution boiling point.

The studied series of the EPR spectra of AR II show transition from LF **E** to DP **S**, but, as temperature increases, it is not possible to attain the bifurcation point ($\omega\tau\sim1$) in the center of the transitional (**I**) spectral-kinetic range (Figure 3). The predicted course of further transformations of the spectral density components is shown by a dashed line.

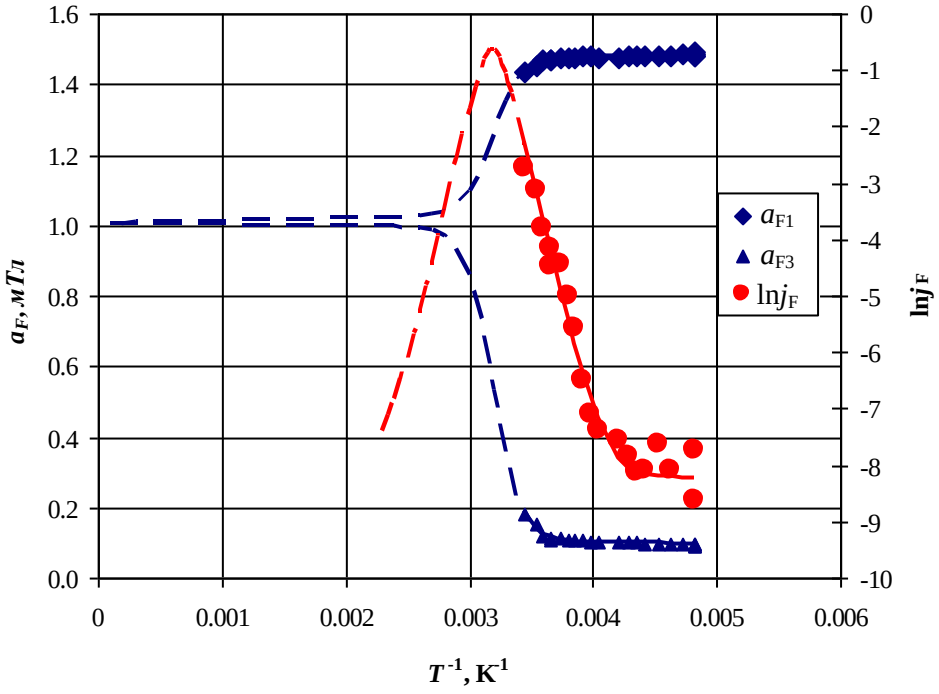

Figure 3. Temperature dependences of the hyperfine splitting constants and broadenings of the central components of the CF_3 group multiplet at the *ortho* position.
[мТл means mT]

Let us present a theoretical derivation of formula (13) based on activation considerations of kinetics. Temperature-reversible spectral transformation **E↔R** corresponds to the thermal process maintaining thermodynamic equilibrium.

Let us present it by the superposition of the counter processes of activation (a) and deactivation (d), i.e., $(E\rightarrow\cdots)_a$ и $(\cdots\leftarrow R)_d$. Such thermal scheme is easily modeled by means of stationary two-directional kinetics. Symbols (E, R) designate the molar quantities of the interconverted LFs E↔R. Let us form the balance of rates taking into account the rate constants of activation and deactivation ($\vec{k}$, $\overleftarrow{k}$).

Let us introduce a time variable *t* and present the rates of the mutually inverse processes, – activation and deactivation – by a system of two kinetic equations:

$$\begin{cases} \dfrac{dE}{dt} = -\vec{k}E + \overleftarrow{k}R, \\ \dfrac{dR}{dt} = -\vec{k}R + \overleftarrow{k}E. \end{cases} \tag{21}$$

Their linear combinations give the following simple and impressive results:

$$\begin{cases} \dfrac{d(E+R)}{dt} = -(\vec{k} - \overleftarrow{k})(E+R), \\ \dfrac{d(E-R)}{dt} = -(\vec{k} + \overleftarrow{k})(E-R) \end{cases} \tag{22}$$

The molar quantities are interrelated by the material balance, i.e.:

$$(E + R) = const. \tag{23}$$

This gives the first condition of stationarity for a dynamic system

$$(\dot{E} + \dot{R}) = 0\,. \tag{24}$$

The observed contour of HFS remains invariable in the course of the measurement. Therefore, there is a second condition of stationarity, for the difference of rates, i.e.,

$$(\dot{E} - \dot{R}) = 0\,. \tag{25}$$

The solution of system (22) reduces itself to algebraic separation of concentration and activation variables:

$$\begin{cases} +(\vec{k} - \overleftarrow{k})(E+R) + (\vec{k} + \overleftarrow{k})(E-R) = 0, \\ -(\vec{k} - \overleftarrow{k})(E+R) + (\vec{k} + \overleftarrow{k})(E-R) = 0. \end{cases} \tag{26}$$

It follows from equations (26) that the current mole fractions of two LFs are associated with the rate constants:

$$\frac{(E-R)}{(E+R)} = x_E - x_R = \mp\frac{(\vec{k} - \overleftarrow{k})}{(\vec{k} + \overleftarrow{k})}\,. \tag{27}$$

Subsequent transformations just refine the obtained result.

The rate constant is the inverse value of correlation time:

$$\begin{cases} \vec{\tau} = \vec{\tau}_\infty \exp(\vec{\varepsilon} T^{-1}) = (\vec{k})^{-1}, \\ \overleftarrow{\tau} = \overleftarrow{\tau}_\infty \exp(\overleftarrow{\varepsilon} T^{-1}) = (\overleftarrow{k})^{-1}. \end{cases} \tag{28}$$

Let us replace T^{-1} using (9), and let us assume that the preexponential multipliers and the modules of activation energy of in activation equations (28) are equal, but differing in sign. Owing to this the dimensionless ratio of the difference and sum of the rate constants in (27) is transformed by substitution of (10) into an antisymmetrized function in the form of hyperbolic tangent:

$$\frac{(\vec{k} - \overleftarrow{k})}{(\vec{k} + \overleftarrow{k})} = \frac{\exp(+\varepsilon\theta) - \exp(-\varepsilon\theta)}{\exp(+\varepsilon\theta) + \exp(-\varepsilon\theta)} = \mathrm{th}(\varepsilon\theta). \tag{29}$$

The molar fractions of the LF are associated with the rate constants of the direct and reverse stages. Therefore, they are also expressed in terms of hyperbolic tangent:

$$\begin{cases} x_E + x_R = 1, \\ x_E - x_R = \mp \text{th}(\varepsilon\theta). \end{cases} \tag{30}$$

We obtain further:

$$\begin{cases} x_E = \frac{1}{2}\left[1 \pm \text{th}(\varepsilon\theta)\right], \\ x_R = \frac{1}{2}\left[1 \mp \text{th}(\varepsilon\theta)\right]. \end{cases} \tag{31}$$

The sign before the fraction in (31) depends on which of the equilibrium constants of splitting changes to the uniform equilibrium value (see Figure 3).

The current value of the isothermal constant of splitting $a(T)$ is formed as the average value. Let us express it using two-component vectors $\{x_E, x_R\}$ and $\{a_E, a_R\}$, the components of which are the molecular ratios and splitting constants of LFs E and R. Let us form their scalar product:

$$a(\theta) = (\{x_E, x_R\} \bullet \{a_E, a_R\}) = x_E \bullet a_E + x_R \bullet a_R \,, \tag{32}$$

which is the required temperature dependence of splitting constants. Each of them changes from its equilibrium value a_E to the common limit a_R. Finally we obtain:

$$a(\theta) = \frac{1}{2}\left[(a_E + a_R) \pm (a_E - a_R)\,\text{th}(\varepsilon\theta)\right]. \tag{33}$$

It is easily seen that formula (33) is the scalar product of two-component vectors analogous to (13):

$$a(\theta) = (\mathbf{A} \bullet \mathbf{T}),$$

$$\mathbf{A} = \{\frac{1}{2}(a_E + a_R), \frac{1}{2}(a_E - a_R)\}, \tag{34}$$

$$\mathbf{T} = \{1, \text{th}(\varepsilon\theta)\}.$$

Vector A consists of the half-sum and half-difference of the theoretical limit values of the splitting constant in the ideal temperature range of its change in the equilibrium thermal process **E↔R**. Vector T consists of the summands of the imaginary component of complex spectral density.

Thus, the independent activation analysis of transformation **E↔R** confirms the key substitution (8), although it seems unusual, even extravagant.

Conclusion

For the first time we obtained in an obvious analytical form the temperature functions of both components of complex spectral density and of the observed constants of isotropic hyperfine splitting in a dynamically modulated multiplet.

In general, as compared to the theory of micromechanical models of relaxation, the hyperbolic "trigonometry" of the temperature-activation representation allows a simple

consideration of the real factors and distortions via semi-empirical modifications [(15) and (20)] of idealized functions (11).

It is shown that these functions are in good agreement with the experimental data, which allows calculating the coordinated activation parameters using the broadening and the splitting constants.

The found activation barrier of the hindered internal motion of AR II attains the extreme value of 37 kJ/mol, which is higher than that of AR I [3]. One of probable causes can be the partial synchronization of the torsion movements of both CF_3 rotors in AR II resulting in an increase of their common moment of inertia and an increase of activation energy. This causes full braking of the CF_3 rotor in the *orto* position at low temperatures, and equilibrium LF E is attained even at 250 K, i.e., 50 K higher than in case of AR I [3]. The activation energies of Brownian rotational diffusion of AR I and II do not differ and are equal to 14.6 and 14.8 kJ/mol, respectively.

References:

1. Polenov E.A., Bozhenko K.V., Shundrin L.A., Smekalkin D.M. // Bull. Rus. Acad. Sci.: Physics. 2004. V. 68. № 7. P. 1206.
2. Smekalkin D.M., Novosadov B.K., Polenov E.A. // Vestnik MITHT. 2007. V. 2. № 5. P. 21–27. (in Russ.)
3. Polenov E.A., Melnikov P.V., Shundrin L.A., Bozhenko K.V. // Bull. Rus. Acad. Sci.: Physics. 2006. V. 70. № 8. P. 1268–1273.
4. Polenov E.A., Shundrin L.A., Melnikov P.V. // Rus. Chem. Bull. 2006. V. 55. № 6. P. 961–967.
5. Polenov E.A., Melnikov P.V., Platonov D.V., Shundrin L.A. // J. Struct. Chem. 2007. V. 48. № 2. P. 245–252.
6. Shundrin L.A., Melnikov P.V., Polenov E.A. // J. Struct. Chem. 2010. V. 50. № 6. P. 1071–1081.
7. Janzen E.G., Gerlock J.L // J. Am. Chem. Soc. 1967. V. 89. № 19. P. 4902–4910.
8. Rogers J.W., Watson W.H. // J. Phys. Chem. 1968. V. 72. № 1. P. 68–74.
9. Melnikov P.V., Polenov E.A. Analizator spektrov. Rekonstrukcija: Gosudarstvennaja registracija programmy dlja JeVM [Spectra analyzer. Reconstruction. State registration of the computer program] № 2014610483. Date 10.01.2014. (in Russ.)